Proceedings of CONF-MSS 2025 Symposium: Machine Vision System
DOI: 10.54254/2755-2721/2025.CH24658

Research on Torque Distribution Strategy for Four-Motor Distributed Drive Vehicles

Jinyi Zhao

School of Mechanical and Materials Engineering, North China University of Technology, Beijing, China
3579789341@qq.com

Abstract. With the global economic development and technological advancement, electric vehicles (EVs) have emerged as a key trend in the automotive industry due to their zero-emission advantage. However, handling stability issues in high-power EVs have become increasingly critical. This study focuses on torque distribution strategies for four-wheel independently driven distributed systems, aiming to enhance vehicle stability and safety by optimizing yaw and sideslip control.A MATLAB simulation model was developed to compare three strategies: no control, average torque distribution, and optimal control. The optimal strategy minimizes the sum of squared tire load ratios under total driving force and yaw moment constraints, using Lagrangian multipliers to derive torque allocation formulas. The average strategy evenly distributes torque while adjusting lateral differences via yaw moments.Simulations based on a linear two-DOF vehicle model and parameters (e.g., mass, wheelbase) under sinusoidal and delayed sinusoidal steering inputs show that the optimal strategy significantly reduces yaw and sideslip angles at 20–30 m/s, with sideslip optimization (93%–99%) and yaw angle reduction (58%–72%) outperforming other methods. At 10 m/s, while yaw angle RMS improvement is limited, sideslip control remains effective.The study confirms that the optimal torque distribution strategy enhances vehicle stability and handling under most conditions by dynamically optimizing wheel torques, providing a theoretical and simulation-based foundation for distributed drive control design.

Keywords: Torque Distribution Strategy, Four-Motor Distributed Drive, Yaw/Slip Angle Optimization, Vehicle Stability Control

1. Introduction

With the rapid advancement of the global economy and technological innovation, the automotive industry has witnessed remarkable growth [1-2]. In 2023, global vehicle sales reached approximately 86 million units, underscoring the sector's substantial scale and societal integration [3]. While automobiles have significantly enhanced daily mobility, traditional internal combustion engine (ICE) vehicles [4-5] face increasingly evident limitations, particularly in energy scarcity and environmental pollution. As a result, the development of zero-emission electric vehicles (EVs) [6] driven by renewable energy has become a dominant trend in the automotive industry, reflecting a critical shift toward sustainability and technological innovation.

DOI: 10.54254/2755-2721/2025.CH24658

Recent advancements in battery and motor technologies have significantly enhanced the performance of EVs. However, the rising popularity of high-power EVs has also led to a surge in traffic accidents caused by improper driver operation or deficiencies in vehicle control systems. Effectively managing these "beasts" has thus become a critical concern. Four-wheel-independently driven distributed drive systems can dynamically and optimally distribute the total demanded torque to each actuator, improving vehicle yaw and sideslip control, thereby enhancing handling stability and safety [7].

In this study, a MATLAB simulation model was developed based on research into four-motor distributed drive systems. The control performance of three strategies—no control, average torque distribution, and optimal torque distribution—was compared. The results demonstrate that optimal torque distribution significantly enhances vehicle stability under most operating conditions [8].

2. Dynamic simulation

2.1. Vehicle motion equation

2.1.1. Optimal control allocation

Objective: Distribute the four-wheel torques T_{fl} , T_{fr} , T_{rl} , T_{rr} to minimize the tire load ratio while satisfying the total driving force and yaw moment requirements.

Optimization Objective Function: Minimize the sum of squared tire load ratios, i.e., minimize energy loss:

$$\min\left(\frac{T_{fl}^{2}}{F_{zfl}^{2}}+\frac{T_{fr}^{2}}{F_{zfr}^{2}}+\frac{T_{rl}^{2}}{F_{zrl}^{2}}+\frac{T_{rr}^{2}}{F_{zrr}^{2}}\right) \tag{1}$$

F_{zi} is the vertical load on each wheel. $\frac{T_i^2}{F_{zi}^2}$ is the squared tire load ratio, reflecting energy dissipation and friction utilization. A higher vertical load increases the tire's friction potential.

Constraints:

1. Total driving force equilibrium: The sum of the torques from all four wheels equals the total driving force:

$$T_{fl}+T_{fr}+T_{rl}+T_{rr}=T_{vx} \tag{2}$$

2. Yaw moment equilibrium: The torque difference between the left and right wheels balances the desired yaw moment:

$$\frac{B_r}{2r}\left(T_{fl}+T_{fr}-T_{rl}-T_{rr}\right)=M_{yaw} \tag{3}$$

B_r is the track width, r is the tire rolling radius, and M_{yaw} is the yaw moment.

The Lagrangian function is constructed using Lagrange multipliers:

$$\mathscr{L}=\sum_i\frac{T_i^2}{\sum F_{zi}^2}+\lambda_1\left(\sum T_i-T_{vx}\right)+\lambda_2\left[\frac{B_r}{2r}\left(T_{fl}+T_{fr}-T_{rl}-T_{rr}\right)\right] \tag{4}$$

λ_1 and λ_2 are Lagrange multipliers.

Taking partial derivatives with respect to each torque and setting them to zero yields:

$$\frac{\partial\mathscr{L}}{\partial T_{fl}}=\frac{2T_{fl}}{F_{zfl}^2}-\lambda_1-\lambda_2\frac{B_r}{2r}=0 \tag{5}$$

DOI: 10.54254/2755-2721/2025.CH24658

$$\frac{\partial \mathscr{L}}{\partial T_{fr}} = \frac{2T_{fr}}{{F_{zfr}}^2} - \lambda_1 + \lambda_2 \frac{B_r}{2r} = 0 \tag{6}$$

$$\frac{\partial \mathscr{L}}{\partial T_{rl}} = \frac{2T_{rl}}{{F_{zrl}}^2} - \lambda_1 - \lambda_2 \frac{B_r}{2r} = 0 \tag{7}$$

$$\frac{\partial \mathscr{L}}{\partial T_{rr}} = \frac{2T_{rr}}{{F_{zrr}}^2} - \lambda_1 + \lambda_2 \frac{B_r}{2r} = 0 \tag{8}$$

The equations reveal symmetry between T_{fl} and T_{rl}, and between T_{fr} and T_{rr}. The front-rear torque ratios are derived as:

$$T_{rl} = \frac{{F_{zrl}}^2}{{F_{zfl}}^2} T_{fl} \tag{9}$$

$$T_{rr} = \frac{{F_{zrr}}^2}{{F_{zfr}}^2} T_{fr} \tag{10}$$

Substituting these into the constraints:

Total driving force constraint:

$$T_{fl}\left(1 + \frac{{F_{zrl}}^2}{{F_{zfl}}^2}\right) + T_{fr}\left(1 + \frac{{F_{zrr}}^2}{{F_{zfr}}^2}\right) = T_{vx} \tag{11}$$

Yaw moment constraint:

$$T_{fl}\left(1 - \frac{{F_{zrl}}^2}{{F_{zfl}}^2}\right) - T_{fr}\left(1 - \frac{{F_{zrr}}^2}{{F_{zfr}}^2}\right) = \frac{2rM_{yaw}}{B_r} \tag{12}$$

Solving these equations gives:

$$T_{fl} = \frac{{F_{zfl}}^2}{{F_{zfl}}^2 + {F_{zrl}}^2}\left(\frac{T_{vx}}{2} - \frac{M_{yaw} r}{B_r}\right) \tag{13}$$

$$T_{fr} = \frac{{F_{zfr}}^2}{{F_{zfr}}^2 + {F_{zrr}}^2}\left(\frac{T_{vx}}{2} + \frac{M_{yaw} r}{B_r}\right) \tag{14}$$

Rear wheel torques are then:

$$T_{rl} = \frac{{F_{zrl}}^2}{{F_{zfl}}^2 + {F_{zrl}}^2}\left(\frac{T_{vx}}{2} - \frac{M_{yaw} r}{B_r}\right) \tag{15}$$

$$T_{rr} = \frac{{F_{zrr}}^2}{{F_{zfr}}^2 + {F_{zrr}}^2}\left(\frac{T_{vx}}{2} + \frac{M_{yaw} r}{B_r}\right) \tag{16}$$

Coefficient Simplification:

$$a_1 = r^2\left({F_{zfl}}^2 + {F_{zrl}}^2\right) \tag{17}$$

$$b_1 = \frac{{F_{zrl}}^2 T_{vx} r^2}{2} - \frac{{F_{zrl}}^2 M_{yaw} r^3}{B_r} \tag{18}$$

a_1 acts as a normalization coefficient, integrating the complex constraints into a single denominator, while b_1 combines the effects of the total driving force and yaw moment on the rear-left wheel into a single numerator term, thereby simplifying the expression for T_{rl}. Then:

$$T_{rl} = \frac{b_1}{a_1} = \frac{{F_{zrl}}^2}{{F_{zfl}}^2 + {F_{zrl}}^2}\left(\frac{T_{vx}}{2} - \frac{M_{yaw} r}{B_r}\right) \tag{19}$$

DOI: 10.54254/2755-2721/2025.CH24658

$\frac{T_{vx}}{2}$ represents equal distribution of total driving force, $\frac{M_{yaw}r}{B_r}$ adjusts the torque difference for yaw control, and $\frac{F_{zrl}{}^2}{F_{zfl}{}^2+F_{zrl}{}^2}$ weights the torque allocation based on vertical loads.

Similarly, we obtain:

$$a_2 = r^2\left(F_{zfr}{}^2 + F_{zrr}{}^2\right) \tag{20}$$

$$b_2 = \frac{F_{zrr}{}^2 T_{vx} r^2}{2} + \frac{F_{zrr}{}^2 M_{yaw} r^3}{B_r} \tag{21}$$

Then:

$$T_{rr} = \frac{b_2}{a_2} = \frac{F_{zrr}{}^2}{F_{zfr}{}^2+F_{zrr}{}^2}\left(\frac{T_{vx}}{2} + \frac{M_{yaw}r}{B_r}\right) \tag{22}$$

2.1.2. Average control allocation

Objective: Distribute the total driving force equally among four wheels, while adjusting the left-right torque difference via M_{yaw} for stability:

$$T_{fl} + T_{fr} + T_{rl} + T_{rr} = T_{vx} \tag{23}$$

$$\frac{B_r}{2r}\left(T_{fl} + T_{fr} - T_{rl} - T_{rr}\right) = M_{yaw} \tag{24}$$

The torque difference $\Delta T = \frac{M_{yaw}r}{B_r}$

The aforementioned equally distributed torque allocation scenario is more suitable for simple, low-dynamic conditions. In this method, an increase in torque demand on one side results in a corresponding decrease on the opposite side. However, this approach has inherent limitations, as it neglects vertical load variations, potentially leading to wheel slippage or inefficient torque distribution. In contrast, the optimal allocation strategy accounts for vertical loads, enabling enhanced dynamic performance and energy efficiency.

2.1.3. Linear two-degree-of-freedom vehicle model

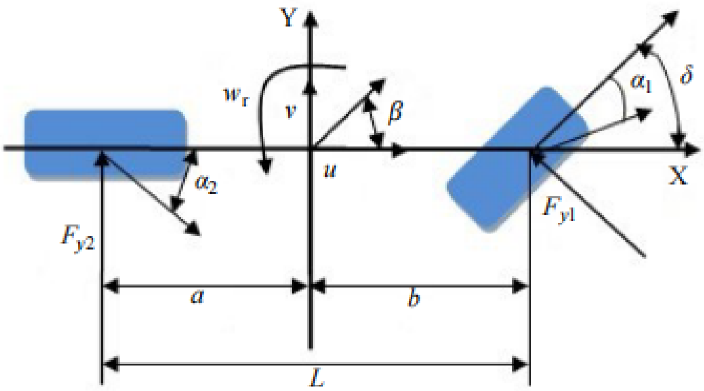

Figure 1: Linear Two-DOF model

Differential Equations:

DOI: 10.54254/2755-2721/2025.CH24658

$$\begin{cases} \dot{\beta} = \frac{k_1+k_2}{mv_x}\beta + \left(\frac{ak_1-bk_2}{v_x} - 1\right)w_r - \frac{k_1}{mv_x}\delta \\ \dot{w}_r = \frac{ak_1-bk_2}{I_z}\beta + \frac{a^2k_1+b^2k_2}{I_z}w_r - \frac{ak_1}{I_z}\delta \end{cases} \tag{25}$$

Vertical Loads:

$$F_{zfl} = mg + \frac{mgL_r}{2L} - \frac{mh_g a_x}{2L} - \frac{mh_g a_y}{2B_r} \tag{26}$$

$$F_{zfr} = mg + \frac{mgL_r}{2L} - \frac{mh_g a_x}{2L} + \frac{mh_g a_y}{2B_r} \tag{27}$$

$$F_{zrl} = mg + \frac{mgL_f}{2L} + \frac{mh_g a_x}{2L} - \frac{mh_g a_y}{2B_r} \tag{28}$$

$$F_{zrr} = mg + \frac{mgL_f}{2L} + \frac{mh_g a_x}{2L} + \frac{mh_g a_y}{2B_r} \tag{29}$$

The wheelbase $L = L_f + L_r$. L_f is the distance from the center of mass to the front axle and L_r is the distance to the rear axle. The total vertical loads on the front and rear axles are $\frac{mgL_r}{L}$ and $\frac{mgL_f}{L}$, respectively.

a_x denotes longitudinal acceleration. $mh_g a_x$ is the moment about the front/rear axle induced by longitudinal acceleration. $\frac{mh_g a_x}{L}$ represents the longitudinal load transfer due to acceleration.

a_y denotes lateral acceleration. $mh_g a_y$ is the moment about the roll axis induced by lateral acceleration. $\frac{mh_g a_y}{B_r}$ represents the lateral load transfer due to cornering.

2.2. Select electric vehicle parameters

The vehicle model and selected vehicle parameters are shown in Figure 2 and Table 1

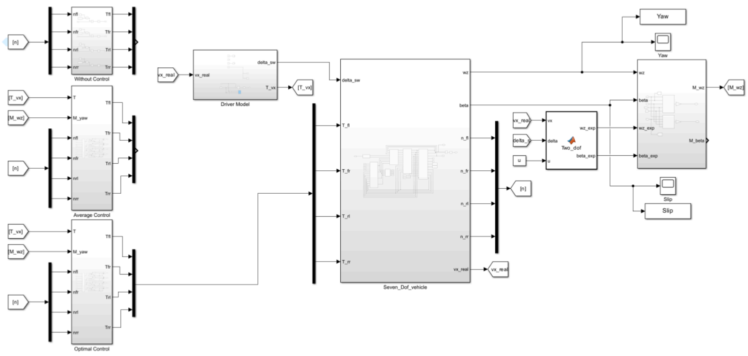

Figure 2: Vehicle model

DOI: 10.54254/2755-2721/2025.CH24658

Table 1: Selected vehicle parameters

Vehicle Parameters	
Projects	Values
Vehicle mass	1765kg
Front axle track	1.6m
Rear axle track	1.6m
CG to front axle distance	1.2m
CG to rear axle distance	1.4m
Wheelbase	2.6m
CG height	0.5m
Yaw moment of inertia	2700kg*m^2
Wheel moment of inertia	2.5 kg*m^2
Cornering stiffness of the front axle	-200e3N/rad
Cornering stiffness of the rear axle	-200e3N/rad

2.3. Analysis of simulation results

The simulation results of the vehicle at 30 m/s with sinusoidal steering wheel angle input (Figure 3) are shown in figure 4 and 5.

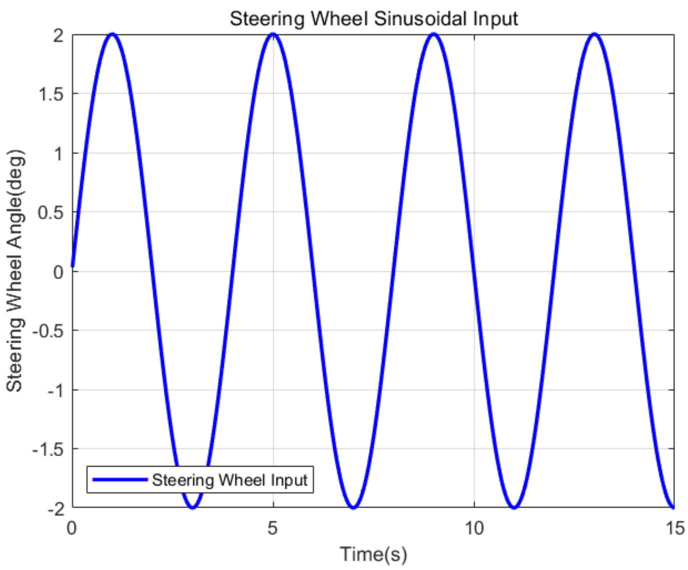

Figure 3: Sinusoidal steering wheel angle input

DOI: 10.54254/2755-2721/2025.CH24658

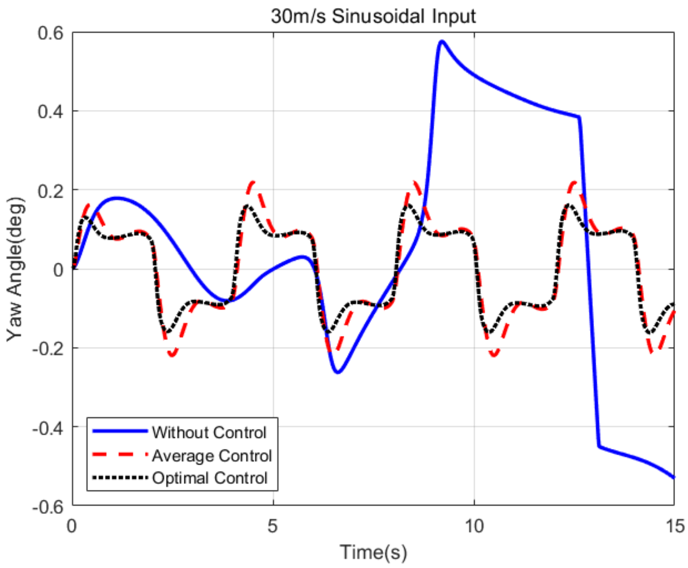

Figure 4: Yaw angle

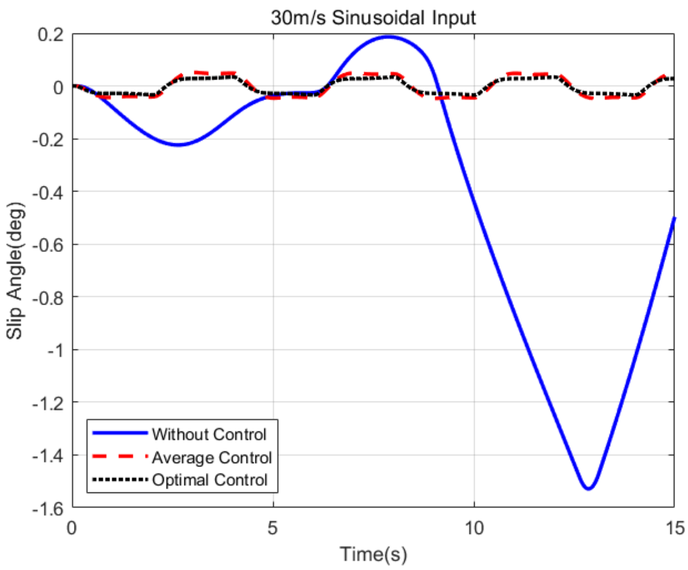

Figure 5: Slip angle

The experimental results under more working conditions are shown in Table 2 and Table 3.

DOI: 10.54254/2755-2721/2025.CH24658

Table 2: Sinusoidal input

Path	Metric	Sinusoidal Input				
		Without Control	Average Control	Improved	Optimal Control	Improved
10m/s	RMS Yaw Angle(deg)	0.1984	0.2316	-16.75%	0.2288	-15.31%
	Max Yaw Angle(deg)	0.4947	0.3254	34.22%	0.3257	34.15%
	RMS Slip Angle(deg)	0.4616	0.0084	98.18%	0.0065	98.59%
	Max Slip Angle(deg)	1.4660	0.0208	98.58%	0.0137	99.06%
20m/s	RMS Yaw Angle(deg)	0.2087	0.1589	23.87%	0.1415	32.19%
	Max Yaw Angle(deg)	0.5744	0.2301	59.94%	0.1929	66.41%
	RMS Slip Angle(deg)	0.2322	0.0338	84.44%	0.0250	89.26%
	Max Slip Angle(deg)	0.8025	0.0455	94.33%	0.0327	95.93%
30m/s	RMS Yaw Angle(deg)	0.3023	0.1268	58.05%	0.1036	65.72%
	Max Yaw Angle(deg)	0.5751	0.2195	61.83%	0.1619	71.86%
	RMS Slip Angle(deg)	0.6379	0.0391	93.88%	0.0264	95.87%
	Max Slip Angle(deg)	1.5284	0.0512	96.65%	0.0345	97.75%

Table 3: Delayed sinusoidal input

Path	Metric	Delayed Sinusoidal Input				
		Without Control	Average Control	Improved	Optimal Control	Improved
10m/s	RMS Yaw Angle(deg)	0.1761	0.2098	-19.12%	0.2067	-17.39%
	Max Yaw Angle(deg)	0.4537	0.3260	28.15%	0.3242	28.56%
	RMS Slip Angle(deg)	0.2219	0.0072	96.77%	0.0055	97.53%
	Max Slip Angle(deg)	0.7501	0.0177	97.64%	0.0116	98.45%
20m/s	RMS Yaw Angle(deg)	0.1880	0.1411	24.92%	0.1265	32.74%
	Max Yaw Angle(deg)	0.4765	0.2294	51.86%	0.1916	59.79%
	RMS Slip Angle(deg)	0.3073	0.0304	90.1%	0.0224	92.7%
	Max Slip Angle(deg)	0.9797	0.0452	95.39%	0.0326	96.67%
30m/s	RMS Yaw Angle(deg)	0.2910	0.1177	59.54%	0.0966	66.8%
	Max Yaw Angle(deg)	0.5989	0.2195	63.36%	0.1620	72.95%
	RMS Slip Angle(deg)	0.5477	0.0359	93.44%	0.0243	95.56%
	Max Slip Angle(deg)	1.5494	0.0508	96.72%	0.0345	97.77%

Based on the data presented in Figures 4, 5 and Tables 2, 3, Under the optimal control, the maximum and RMS values of the vehicle's yaw angle and slip angle are significantly improved compared to those under average control and no control. This demonstrates that the optimal control effectively enhances vehicle stability and handling performance at speeds of 20 m/s and 30 m/s under both sinusoidal and delayed sinusoidal steering inputs.

However, the results indicate that the proposed algorithm does not achieve optimal control over the yaw angle RMS value in certain scenarios, such as at a speed of 10 m/s with sinusoidal or delayed sinusoidal steering inputs. Nevertheless, its impact on the yaw angle remains marginal, while the maximum value is substantially optimized. Therefore, it can still be concluded that vehicle stability is improved to some extent even under these conditions.

DOI: 10.54254/2755-2721/2025.CH24658

3. Conclusion

This study conducts a systematic analysis of torque distribution strategies for four-motor distributed drive vehicles, revealing the influence mechanisms of different control strategies on vehicle stability through theoretical modeling and simulation verification. The research establishes an optimal torque distribution model aiming to minimize the sum of squared tire load ratios. By incorporating constraints of total driving force and yaw moment, analytical expressions for four-wheel torques are derived using the Lagrangian multiplier method, and compared with the average distribution strategy and uncontrolled state. Simulation results show that under sinusoidal and delayed sinusoidal steering inputs, the optimal control strategy significantly enhances vehicle dynamic stability:

High-speed conditions (20–30 m/s): The maximum yaw angle is reduced by 58%–72%, and the root mean square (RMS) value is reduced by 58%–66%; the maximum sideslip angle is optimized by 93%–98%, and the RMS value is optimized by 89%–96%, effectively suppressing the risk of excessive yaw and sideslip during vehicle steering. Low-speed conditions (10 m/s): Although the optimization effect on the yaw angle RMS is limited (slightly increased in some scenarios), the sideslip angle is still optimized by 96%–99%, indicating the universal applicability of the optimal strategy for dynamic management of tire grip.

The study further finds that the average distribution strategy tends to cause uneven torque distribution under high-dynamic conditions due to neglecting differences in tire vertical loads. In contrast, the optimal strategy achieves collaborative optimization of driving force and yaw moment by introducing load weight coefficients, significantly improving tire friction utilization and energy efficiency.

In summary, the optimal torque distribution strategy effectively enhances vehicle handling stability and safety under most working conditions by dynamically adjusting four-wheel torques, providing a theoretical basis for the design of control algorithms for distributed drive vehicles. Future research can further integrate real-time road parameter sensing to optimize the robustness of the torque distribution model and adapt to complex driving environments.

References

[1] A fast and parametric torque distribution strategy for four-wheel-drive energy-efficient electric vehiclesDizqah, A.M.; Lenzo, B.; Sorniotti, A.IEEE Trans Ind Electron, v 63, n 7, p 4367-4376, 2016

[2] Torque optimization control for electric vehicles with four in-wheel motors equipped with regenerative braking systemXu, W.; Chen, H.; Zhao, H.Mechatronics, v 57, p 95-108, 2019

[3] Road surface recognition based slip rate and stability control of distributed drive electric vehicles under different conditionsHongbo, W.; Boyang, Z.; Jinfang, H.Proc IMechE, Part D: J Automob Eng, v 237, n 10-11, p 2511-2526, 2023

[4] All-wheel-drive torque distribution strategy for electric vehicle optimal efficiency considering tire slipCao, K.; Hu, M.; Wang, D.IEEE Access, v 9, p 25245-25257, 2021

[5] Cooperative control of trajectory tracking and lateral stability of distributed driven electric vehicleZhang, Z.; Jin, B.J Chang Univ Sci Technol Nat Sci, v 20, n 6, p 159-169, 2023

[6] An integrated control strategy of path following and lateral motion stabilization for autonomous distributed drive electric vehiclesZou, Y.; Guo, N.; Zhang, X.Proc IMechE, Part D: J Automob Eng, v 235, n 4, p 1164-1179, 2021

[7] A supervisory control strategy of distributed drive electric vehicles for coordinating handling, lateral stability, and energy efficiencyGuo, N.; Zhang, X.; Zou, Y.rans Transp Electrification, v 7, n 4, p 2488-2504, 2021

[8] MPC-based integrated control of trajectory tracking and handling stability for intelligent driving vehicle driven by four hub motorZhai, L.; Wang, C.; Hou, Y.IEEE Trans Vehicular Technol, v 71, n 3, p 2668-2680, 2022